

# AAV Aggregate Quantitation and Identification with the Aura System

## Introduction

Adeno-associated viruses (AAVs) have transformed gene therapies by enabling the targeted delivery of curative genetic payloads<sup>1</sup>. However, the amount of AAV material available is consistently in short supply due to its inherently expensive, time-consuming, and laborious production process<sup>1</sup>. Regardless, critical quality attributes still need to be measured throughout development. Subvisible particles are perhaps the most important parameter to monitor because they lead to adverse immunogenicity events. Thus, this data must be provided to the FDA during the review process<sup>2</sup>. Additionally, measuring the stability of the capsid is an indicator of the shelf life and efficacy of the product.

Halo Labs' Aura™ platform is the first ultra-low-volume, subvisible particle analysis system that quantitatively characterizes the stability of different AAV serotypes with as little as 5 µL. This application note demonstrates how several AAV serotypes tend to form large, subvisible aggregates that cannot be predicted using other techniques. It explores the stability and subvisible particle formation in AAV2, AAV5, and AAV8 under different stress conditions and compare the results to stability predictions made by differential scanning calorimetry. In addition, it analyzes the nature of the subvisible aggregates using complete morphological analysis and Fluorescence Membrane Microscopy (FMM) using as low as 10 µL per AAV sample.

## Material and Methods

AAV2, AAV5, and AAV8-containing CMV-driven GFP expression cassettes were obtained from Vigene Biosciences (Rockville, MD USA). The virus was suspended in PBS + 0.01% pluronic F68 surfactant. Viral samples were thawed at room temperature (RT) and then split into separate tubes to facilitate the various stress conditions:

- 1 Non-stressed control samples stored at 4 °C after thawing
- 2 Thermally-stressed samples heated at 73 °C for 2 hours
- 3 Rotation samples vortexed for 5 minutes, rotated for 2 hours, then vortexed for 5 minutes
- 4 Freeze-thaw samples subjected to an additional round of freeze-thaw at -20 °C and RT
- 5 30 µL ETFE pipetted on top of a 30 µL droplet of non-stressed AAV
- 6 Water for injection (WFI) control samples where Thoflavin-T (ThT) was pipetted over a membrane previously processed with water

The 30 µL of the various samples were loaded in triplicate on a backgrounded black Halo Labs plate. Samples were imaged using both brightfield (Background Membrane Imaging – BMI) and fluorescence (Fluorescence Membrane Microscopy – FMM) technology. ThT was used to specifically stain protein aggregates in the samples for fluorescence detection with FMM.

## Results

Subvisible particle aggregation was observed as a function of serotype and stress conditions with as little as 10  $\mu\text{L}$  per sample (Figure 1). When unstressed AAV samples (samples processed and measured directly from the vial) were compared to each other, the AAV2 (Figure 1a) sample contained less subvisible particles compared to the AAV5 (Figure 1b) and AAV8 (Figure 1c) samples, respectively. Increased levels of protein aggregation were observed in all AAV samples after stressing the samples at 73  $^{\circ}\text{C}$  for 2 hours, though each serotype produced aggregates with different morphologies. The stressed AAV2 produced well-defined small to large granular particles (Figure 1d) while stressed AAV5 contained large fibrillar structures

(Figure 1e). The stressed AAV8 sampled (Figure 1f) denatured into a film-like matrix that spread throughout the membrane, resulting in no discernable subvisible particles but showing complete sample degradation.

The particles larger than 2  $\mu\text{m}$  in equivalent circular diameter were used to evaluate particle aggregation quantitatively (Figure 2). Each sample well was measured in triplicate, using a total of 30  $\mu\text{L}$  of sample per well. The unstressed AAV2 produced the lowest counts, followed by the unstressed AAV5 and unstressed AAV8 samples. While AAV5 and AAV8 appear to produce a similar number of particles on average, AAV8's variance was significantly higher, likely due to the matrix-like degradation captured in Figure 1f. The samples stressed for 2 hours at 73  $^{\circ}\text{C}$

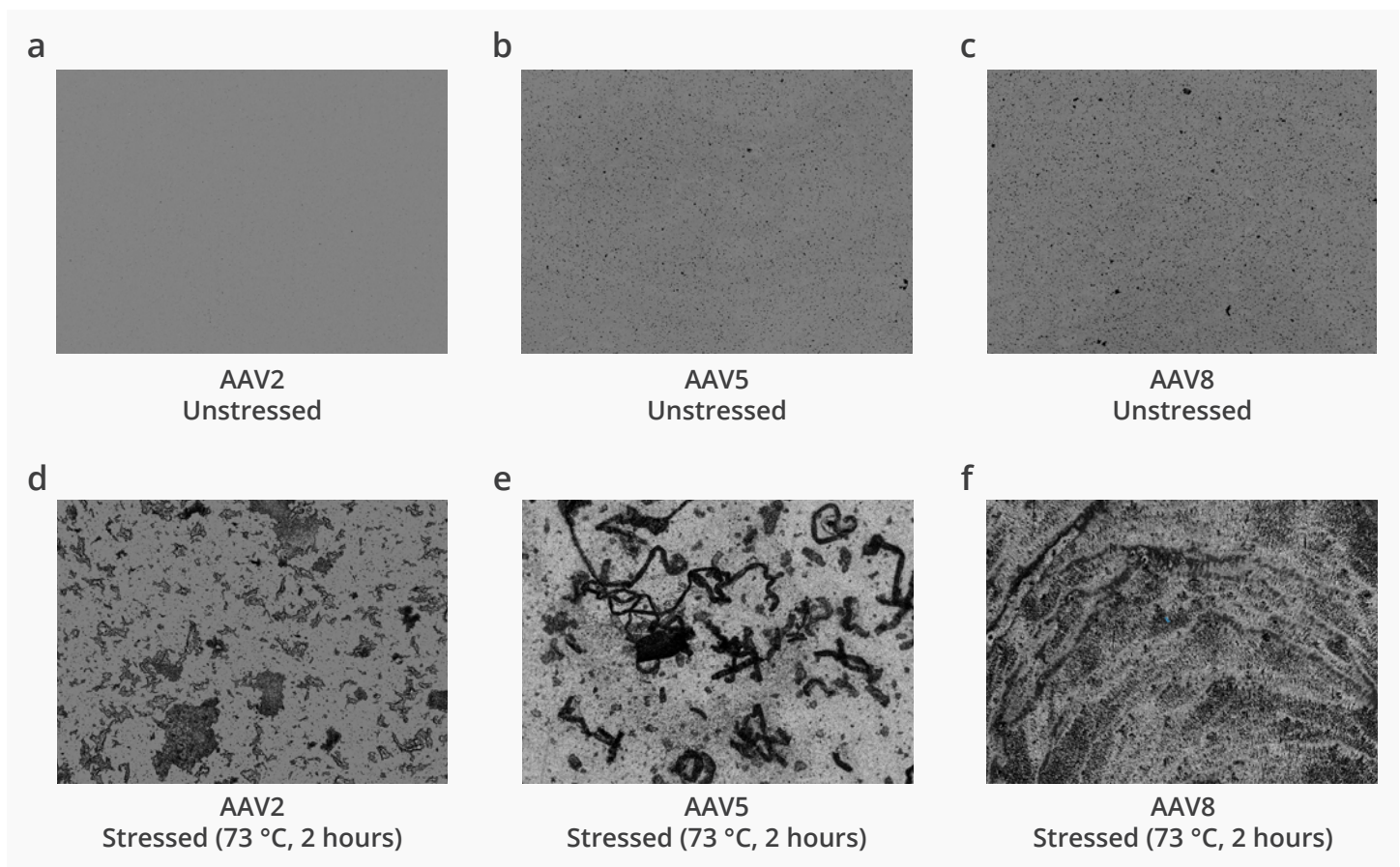


**Figure 1:** Brightfield membrane images for different AAV serotypes. (a–c) Unstressed AAV2, AAV5, and AAV8 samples. (d–f) Thermally-stressed (73  $^{\circ}\text{C}$ , 2 hours) AAV2, AAV5, and AAV8 samples. All images were magnified to 100  $\mu\text{m}$ .

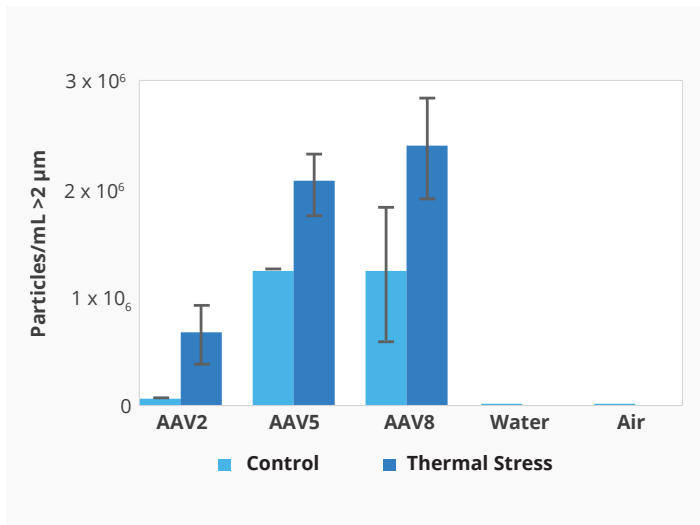


**Figure 2:** Quantitative counts for different AAV serotypes with and without thermal stress.

also exhibited a similar pattern. AAV2 produced the lowest number of particles, followed by AAV5 and AAV8 in that order. These last two samples showed significant aggregation with over  $2.0 \times 10^6$  particles/mL. The negative air and water controls produced almost no counts.

The AAV2 sample was then stressed under different conditions and analyzed using combined brightfield and fluorescence images (Figure 3). AAV2 was picked as a model since it exhibited the lowest thermal stability, as will be discussed in the discussion section below. There was almost no subvisible particle formation in the unstressed sample and WFI control (Figure 3a, e) while strong fluorescence was observed from the granular subvisible aggregates (Figure 3b). This strong Thioflavin T fluorescence (red) indicates that there is a very significant

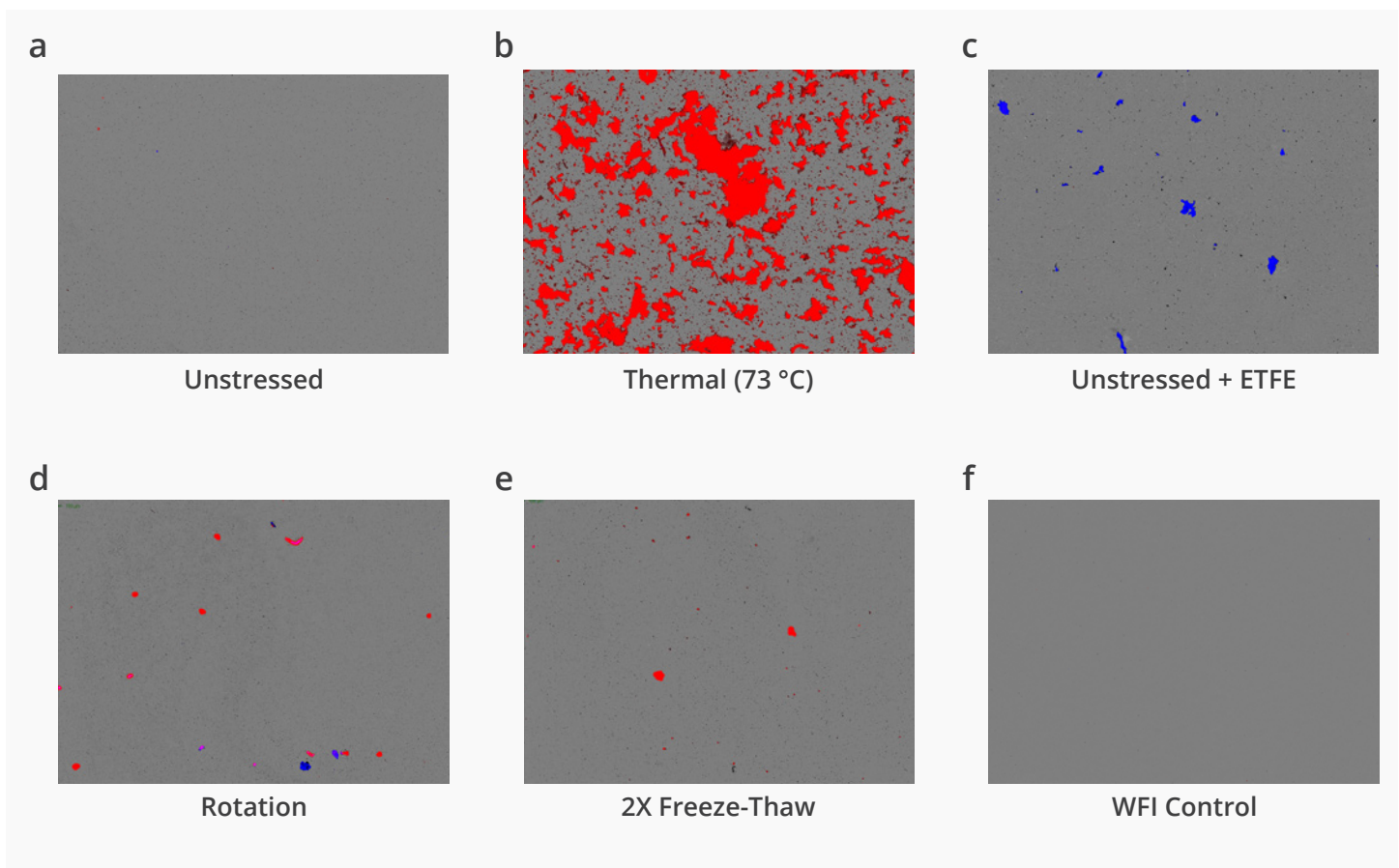


**Figure 3:** Combined Brightfield (blue) & Fluorescence (red) images for AAV2 samples under several stress conditions. (a) No stress (b) Thermal (c) No stress + ETFE (d) Rotation (e) Freeze-Thaw and (f) WFI Control. All images were magnified to 100 μm.

aggregation of the protein capsids in the heat-stressed samples; to the point where they even become visible (Equivalent Circular Diameter (ECD)  $>100 \mu\text{m}$ ). When the unstressed sample with NIST ethylene tetrafluoroethylene (ETFE) plastic protein aggregate mimics filtered over the original unstressed sample (Figure 3c) was analyzed, no ThT fluorescence was observed from the plastic particles though there was a strong out of plane SIMI scattering (blue) signal, indicating that these particles protrude out of plane, unlike their AAV counterparts. The rotational stress samples showed very little capsid aggregation (Figure 3d), but these aggregates did display strong side scattering as captured by the purple particles in the image. Low levels of aggregate formation were also observed in samples subjected to two cycles of freeze-thawing (Figure 3e).

The no stress, thermal stress, rotation, and freeze-thaw samples were further analyzed quantitatively using counts/mL (Figure 4a) and membrane coverage (Figure 4b) as readouts. While count monitors the discrete number of particles counted for a given size range, membrane coverage indicates the total percentage of the membrane area that was covered in particulate material. Both analysis modalities produced the same results across all conditions within experimental error: the unstressed sample produced the least number of particles and  $<1\%$  membrane coverage, while the thermally stressed sample produced more than 600,000 particles/mL that were  $\geq 2 \mu\text{m}$  and covered 16% of the membrane in particulate material. Rotation and freeze-thawing stress exhibited slightly more than 50% more counts than the unstressed sample, with the results between these two stresses falling within experimental error. A more detailed analysis (not shown) of the particulate counts between the rotated and freeze-thaw samples reveals that the rotated sample revealed four times as many very large particles ( $\geq 25 \mu\text{m}$ ) compared to the freeze-thawed samples, which would have greater repercussions for USP-type lot release requirements.

## Discussion

The Aura system detects and distinguishes the particles formed in different AAV serotypes, both in unstressed and stressed samples. The data generated demonstrated that neat, unstressed samples contain visible aggregates and that each AAV serotype forms different types of aggregates, from granular (AAV2), through fibrillar (AAV5) to fully denatured films (AAV8), when they were thermally stressed. Thermally stressing the AAV2 samples at  $73 \text{ }^\circ\text{C}$  for 2 hours produced a significantly lower number of particles compared to the AAV5 and AAV8 samples, respectively.

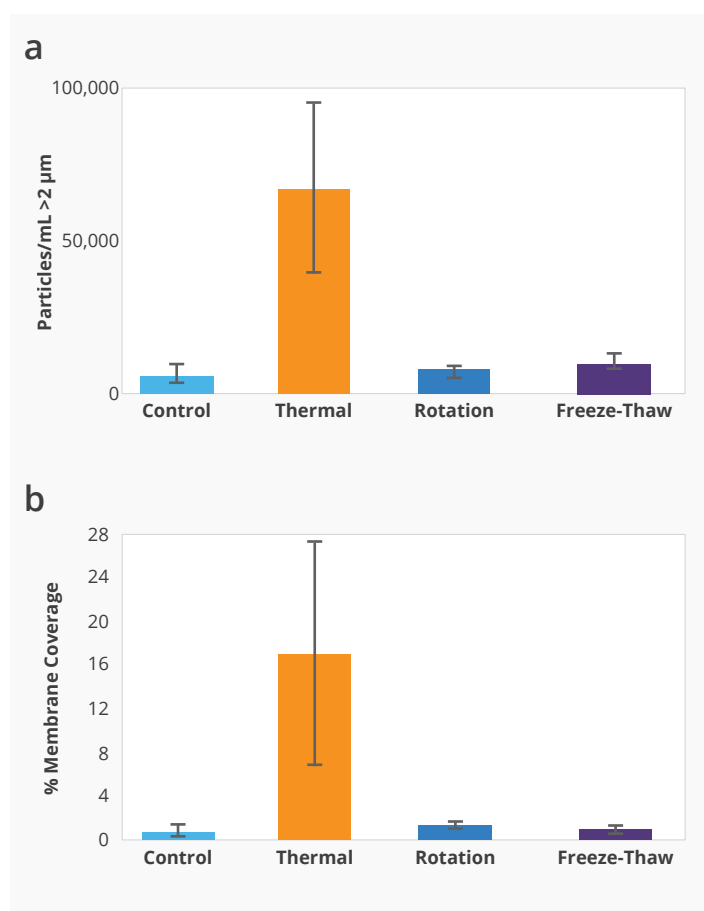


**Figure 4:** AAV2 particle data for several stress conditions. (a) Particle ECD  $\geq 2 \mu\text{m}$  and (b) Membrane coverage.

Bennett *et al.*<sup>3</sup> used differential scanning fluorimetry (DSF) to help assess the thermal stability of several AAVs. Their DSF analysis measured the following melting temperatures ( $T_m$ ): AAV2: 67 °C, AAV5: 89 °C and, AAV8: 73 °C. Therefore, it takes the most energy to thermally denature AAV5, while AAV2 should be the least stable at 67 °C. 73 °C was chosen as the  $T_m$  for AAV8, as the thermal stress condition in order to evaluate the three serotypes at, below, or above their  $T_m$ . TABLE 1 compares the  $T_m$  stability prediction values against the true measured particulate formation detected by the Aura system.

There was no direct correlation between  $T_m$  data and subvisible-particle formation for any of these serotypes. AAV2, which is supposedly the least thermally-stable molecule according to DSF, was the serotype that exhibited the lowest number of particles. This measurement was also corroborated by the membrane coverage measurement. On the other hand, AAV5 was supposedly the most thermally-stable but actually showed more severe aggregation compared to AAV2. AAV8 was supposedly the most thermally-stable but showed the largest number of particles in its native state, and full denaturation in its thermally-stressed state. In addition, the images captured using the Aura system revealed important information that can give clues to the mechanism of aggregate formation since fibrillation and granulation are inherently different degradation mechanisms.  $T_m$  predicts the temperature at which a large molecule starts to unfold, but this does not necessarily correlate or predict dimerization or aggregation in the nano or subvisible scale. In other words,  $T_m$  does

	AAV2	AAV5	AAV8
nanoDSF ( $T_m$ )	Low	High	Medium
BMI (Diameter)	High	Medium	Low

**TABLE 1:** Comparison of thermal stability measurements using the Aura instrument and nanoDSF.

not predict particle formation, it is not a surrogate for, and cannot replace subvisible data.

Fluorescent Membrane Microscopy (FMM) using Thioflavin T in the Aura system was used to further investigate particle formation by AAV2 under several stress conditions. The data generated showed that >90% of the particle measured were capsid aggregates. While morphologically very similar to protein aggregates, ETFE is not labeled with ThT, displaying the dye's specificity for proteinaceous aggregates. Furthermore, Figure 4 shows that the Aura instrument can measure particulate content and rank formulations both measuring discrete particles and membrane coverage with all conditions trending the same and within error between both types of measurements. This is very important since not all samples will form discrete particles. Particle formation very much depends on the type of molecule, buffer, excipient, and stress conditions. Membrane coverage is a surrogate measurement for total particulate content, which is crucial in formulation analysis because USP 788 is ultimately designed to limit the intake of total particulate content (matter). Membrane coverage is potentially a better way of quantifying the amount of undesired material produced by a given sample.

The Aura platform delivered both quantitative and qualitative protein aggregation information for several AAV serotypes under different conditions with volumes as low as 10  $\mu$ L per sample. In comparison, this is <30X the volume typically required with the most advanced low volume flow imager and <1000X lower volume than light obscuration systems. The ability to image brightfield (BMI) and fluorescence (FMM) images at the same time also defines what is protein and what is not in the ThT-stained samples. The Aura system helps characterize your AAV samples with the lowest volume requirements, the highest throughput (<1 minute/sample) and reveals the greatest insights into their stability. 

## References

1. Wang D, Tai PW, Gao G. Adeno-Associated Virus Vector as a Platform for Gene Therapy Delivery. *Nat Rev Drug Discov.* 2019 May;18(5):358-78.
2. Test for Particulate Contamination: Subvisible Particles General Chapter Guidance for Industry. *USDHHS and FDA* 2017.
3. Bennett A, Patel S, Mietzsch M, Jose A, Lins-Austin B, Jennifer CY, Bothner B, McKenna R, Agbandje-McKenna M. Thermal Stability as a Determinant of AAV Serotype Identity. *Mol. Ther. Methods Clin Dev.* 2017 Jul 24;6:171-182.

